Electrical Power and Energy Systems 91 (2017) 71–79

Contents lists available at ScienceDirect

Electrical Power and Energy Systems

journal homepage: www.elsevier.com/locate/ijepes

Phase shifting transformer model for direct approach power flow studies

José M. Cano *, Md. Rejwanur R. Mojumdar, Joaquín G. Norniella, Gonzalo A. Orcajo

Department of Electrical Engineering, University of Oviedo, Spain

ARTICLE INFO

Article history:
Received 11 January 2017
Received in revised form 2 March 2017
Accepted 12 March 2017
Available online 22 March 2017

Keywords:
Direct approach method
Phase shifting transformer
Power flow
Weakly-meshed network

ABSTRACT

This proposal is intended to extend the field of application of an extremely efficient power flow algorithm used in radial and weakly meshed grids, the so-called Direct Approach (DA) method. In this work the method is broadened with the possibility of handling shunt admittances, transformers with taps, and phase shifting transformers. While the integration of the two former elements in the DA solver is quite straightforward, the use of phase shifting transformers is far from obvious due to their inherent non-symmetrical admittance matrix. Thus, a model for phase shifting transformers is proposed in this contribution, which allows the use of the DA method in grids that include such devices. A set of case studies is conducted in the contexts of a balanced industrial grid and a standard testbed to demonstrate the validity of the proposal.

1. Introduction

Power flow solvers are an essential tool in the operation and planning of power systems. They allow the assessment of voltage profiles, power flows and losses in the grid, and thus, they are crucial to detect unacceptable voltage deviations and identify overloaded components. Furthermore, power flow algorithms are used to conduct reliability studies and foresee the impact of future demand [1,2].

The most traditional power flow methods such as Newton-Raphson and Gauss-Seidel, used widely in transmission systems, do not offer the best performance and robustness when applied to the distribution level [3]. This is due to the especial nature of the distribution network, characterized by a radial or weakly meshed topology and a high R/X ratio. Several approaches have been proposed in order to deal with these particular features, such as the implicit Z-bus Gauss method [4] and backward-forward sweep methods [5,6]. In the latter group, a very efficient formulation called the direct approach (DA) was proposed in [7]. The DA method avoids the time-consuming tasks of LU factorization and forward and backward substitution of the Jacobian or admittance matrices, which are a commonplace in traditional formulations. The characteristics of DA method make it ideal for real-time applications in the smart grid context. In [8], the DA solver is used in the core of an optimal power flow (OPF) algorithm to provide references to a distribution FACTS in an industrial grid. High update rates are needed in this type of applications and the DA solver accommodates perfectly to this requirement.

The three-phase approach used in [7] takes series self-impedances and mutual couplings into consideration; however, shunt admittances are neglected. Even if that assumption can be enough to run a power flow analysis at the lowest voltage levels of the distribution grid, characterized by short-length lines and untapped transformers, ignoring shunt admittances strongly limits the application of the method to higher voltage levels. The extension of the method to accommodate medium-length lines and transformers with tap changers in a balanced environment is presented in this paper. Though no previous references to this use have been found, its application is fairly straightforward.

In a pure radial grid, a post-processing of the voltage phase angles after the application of the power flow solver is enough to account for the transformer phase shift. However, if a weakly meshed grid is to be considered, this method is no longer valid. Thus, a model of the phase shifting transformer, both to consider specific devices used to control the active power flow in the loop and to include the phase shift of common power transformers, is mandatory. Modeling of phase shifting transformers in power flow studies is a non-trivial problem, as they cannot be represented by a pi-equivalent component due to their inherent asymmetric admittance matrix [1]. A set of different phase shifting transformer models is available for application in various fields of study, to both steady state [9–13] and transient simulation [14]. In [15], a survey on phase shifting transformer models for steady state analysis is presented; however, none of them are expressed in a suitable form to be embedded in the DA solver. In this work, a new model is proposed to overcome this limitation.

* Corresponding author.
E-mail address: jmcano@uniovi.es (J.M. Cano).

http://dx.doi.org/10.1016/j.ijepes.2017.03.007
0142-0615/

The DA method, as described in [7], is presented in Section 2 for the benefit of the reader. Section 3 presents a straightforward method to include shunt admittances in the DA solver. Thus, those components capable of being represented by pi-equivalent models, such as medium-length lines and transformers with tap changers, can be easily included in the problem. In Section 4, the new phase shifting transformer model is presented together with minor modifications to be performed in the DA algorithm. Three case studies are presented in Section 5 in order to illustrate the implementation procedure and demonstrate the validity of the proposal. Finally, Section 6 summarizes the most important results of this study.

2. Direct approach power flow

The method to be proposed in this contribution is based on the DA formulation of the power flow problem [7]. This is a technique, especially designed for radial networks, inspired by well-known backward-forward sweep methods such as Ladder Iterative Technique [6]. DA provides a very compact vectorized formulation with excellent computational and convergence characteristics.

In the application of DA to balanced grids, lines and transformers are modeled as series impedances, z_{ik}, as it is shown in Fig. 1. The equivalent bus current injection vector, $\boldsymbol{I_g}$, is calculated from the power injection at each bus, i, given the estimation of the bus voltage vector $\boldsymbol{V}$ at iteration (n) as

$$I_{gi}^{(n)} = \frac{P_i - jQ_i}{conj(V_i^{(n)})}. \tag{1}$$

Assuming a radial grid, the branch current vector can be calculated as

$$\boldsymbol{B}^{(n)} = \mathbf{BIBC} \cdot \boldsymbol{I_g}^{(n)}, \tag{2}$$

where **BIBC** is the so-called bus-injection to branch-current matrix. The entry $BIBC_{bi}$ equals 1 if the current injection of node i contributes to the branch current B_b, and equals 0 otherwise. Finally, a better approximation to the voltage profile can be obtained from

$$\boldsymbol{\Delta V}^{(n+1)} = \mathbf{BCBV} \cdot \boldsymbol{B}^{(n)}, \tag{3}$$

where **BCBV** is the branch-current to bus-voltage matrix. The entry $BCBV_{ib}$ equals the series impedance of branch b if that branch is in the path from node i to the slack bus, and equals 0 otherwise. $\boldsymbol{\Delta V}$ is a vector with the voltage of the slack bus referred to the different bus voltages. An improved approximation to the state variables is subsequently obtained by

$$\boldsymbol{V}^{(n+1)} = \boldsymbol{V_s} - \boldsymbol{\Delta V}^{(n+1)}, \tag{4}$$

where $\boldsymbol{V_s}$ is a column vector with the slack bus voltage at each entry.

Starting from a flat voltage profile, the solution of the distribution power flow is reached by solving (1)–(4) iteratively up to a specified convergence threshold.

In order to include the treatment of meshes in the network, Teng [7] proposes minor modifications to be conducted in the definition of **BIBC** and **BCBV** and in the solution technique. A brief summary of these changes can be described as:

- Specific branches are selected to break the meshed grid into a radial network. Then, new entries are included in the current injection vector to account for the currents at the selected branches, i.e. $[\boldsymbol{I_g B}_{\text{new}}]^T$.
- The **BIBC** matrix is built as in the base case, by considering the currents of the branches used to break the network as additional current injections. However, entries with the value -1 appear now to account for the contribution of the receiving node of the branches used to break the network due to the inverted current reference. Notice that the double-sided contribution of the sending and receiving nodes of a branch used to break the network, B_c, to the current of those branches upstream from the first common parent node, B_b, is null, as they have the same value but opposite references.
  Additionally, new rows are added to the **BIBC** matrix with a single non-null entry in order to identify the currents of the branches used to break the network. Taking all this into account the modified **BIBC** matrix can be obtained as

$$\begin{bmatrix} \boldsymbol{B} \\ \boldsymbol{B}_{\text{new}} \end{bmatrix}^{(n)} = \mathbf{BIBC} \cdot \begin{bmatrix} \boldsymbol{I_g} \\ \boldsymbol{B}_{\text{new}} \end{bmatrix}^{(n)}. \tag{5}$$

- The **BCBV** matrix is built as in the base case, but a new row is added for each loop in the grid to account for KVL. The impedances included in the entries of the new rows of the matrix are signed positive or negative according to the reference of the current at the different branches. Then, (3) is reformulated as

$$\begin{bmatrix} \boldsymbol{\Delta V} \\ 0 \end{bmatrix}^{(n+1)} = \mathbf{BCBV} \cdot \begin{bmatrix} \boldsymbol{B} \\ \boldsymbol{B}_{\text{new}} \end{bmatrix}^{(n)}. \tag{6}$$

- By using (5) and (6) and rewriting the resulting matrix, it follows that

$$\begin{bmatrix} \boldsymbol{\Delta V} \\ 0 \end{bmatrix}^{(n+1)} = \mathbf{BCBV} \cdot \mathbf{BIBC} \cdot \begin{bmatrix} \boldsymbol{I} \\ \boldsymbol{B}_{\text{new}} \end{bmatrix}^{(n)} = \begin{bmatrix} \boldsymbol{A} & \boldsymbol{P} \\ \boldsymbol{M} & \boldsymbol{N} \end{bmatrix} \begin{bmatrix} \boldsymbol{I} \\ \boldsymbol{B}_{\text{new}} \end{bmatrix}^{(n)}.$$

The application of Kron reduction to (7) leads to

$$\boldsymbol{\Delta V}^{(n+1)} = (\boldsymbol{A} - \boldsymbol{M}^T \boldsymbol{N}^{-1} \boldsymbol{M}) \boldsymbol{I_g}^{(n)}. \tag{7}$$

The iterative use of (1), (7) and (4), in this order, allows the application of the DA method to weakly meshed grids.

3. Including pi-equivalent models

The DA method in [7] models the lines and transformers in balanced systems by simple series impedances. While this is acceptable for short-length lines and untapped transformers, minor

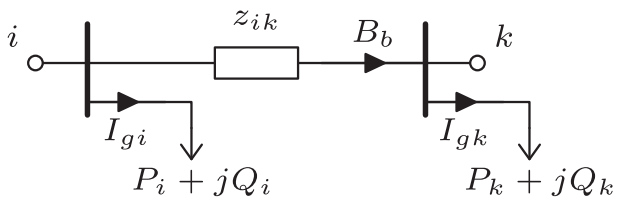

Fig. 1. Scheme used in the DA method.

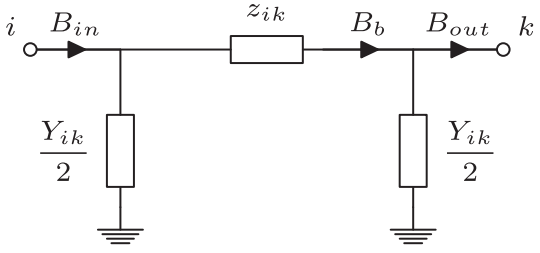

Fig. 2. Pi-equivalent line model.

modifications must be included in the method in order to deal with other common device models.

By considering a pi-equivalent model as the one shown in Fig. 2, medium-length lines with series impedance z_{ik} and total lumped shunt admittance Y_{ik} can be included in the DA method. In this case, an intermediate variable arises, B_b, which is to be included in the branch current matrix $\boldsymbol{B}$. The current injection vector, $\boldsymbol{I_g}$, is now replaced in (2) by an augmented vector $\boldsymbol{I}$ that includes the currents drawn by the shunt admittances as

$$\boldsymbol{I}^{(n)} = \boldsymbol{I}_{\boldsymbol{g}}^{(n)} + \mathbf{Y_B} \circ \boldsymbol{V}^{(n)}, \tag{8}$$

where $\circ$ is the Hadamard product and $\mathbf{Y_B}$ is the bus admittance vector. The sending and receiving end currents, B_{in} and B_{out}, do not appear explicitly in the formulation, but can be subsequently obtained from the state variables by

$$B_{in} = B_b + \frac{Y_{ik}}{2} V_i, \tag{9}$$

$$B_{out} = B_b - \frac{Y_{ik}}{2} V_k. \tag{10}$$

Once the structure in Fig. 3 is adopted, no further modifications are required in the DA method if z_{ik} is used within the **BCBV** matrix.

Even more important than medium-length lines in radial grids is the inclusion of tap changing transformers in the DA solver. The latter devices are massively used along the power system and are of particular importance in the regulation of voltages in radial grids, to which the DA method is specifically devoted. Considering a tap changing transformer as in Fig. 4, where Y_{sc} stands for its short circuit admittance and a represents the regulation between the primary and secondary voltages, the following equations apply

$$V_i = aV_p = a\left(\frac{B_{out}}{Y_{sc}} + V_k\right), \tag{11}$$

$$B_{out} = aB_{in}. \tag{12}$$

As it is well established in [16], from (11) and (12) the tap changing transformer can be represented through a pi-equivalent model as in Fig. 5, which accounts for the nodal equations of the machine

$$B_{in} = \frac{1}{a^2} Y_{sc} V_i - \frac{1}{a} Y_{sc} V_k, \tag{13}$$

$$-B_{out} = -\frac{1}{a} Y_{sc} V_i + Y_{sc} V_k. \tag{14}$$

Using the same methodology described for pi-equivalent lines, the inclusion of tap changing transformers in the DA method is thus achieved. Notice that, in this case, the input and output currents of the transformer can be derived from the state variables as

$$B_{in} = B_b + \frac{1-a}{a^2} Y_{sc} V_i, \tag{15}$$

$$B_{out} = B_b - \frac{a-1}{a} Y_{sc} V_k. \tag{16}$$

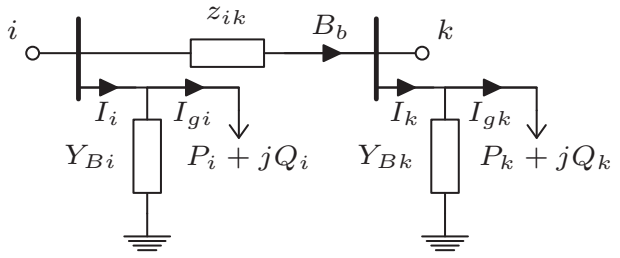

Fig. 3. Modified scheme for the DA method.

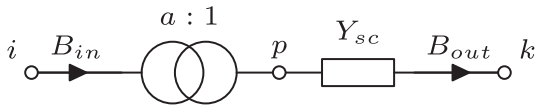

Fig. 4. Equivalent circuit for the tap changing transformer.

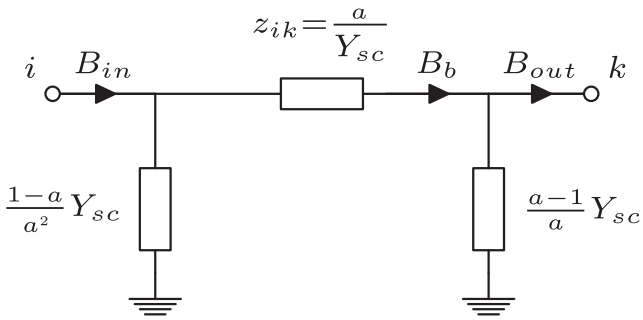

Fig. 5. Pi-equivalent model of the tap changing transformer.

4. Phase shifting transformer model

Phase shifting transformers cannot be represented through a pi-equivalent model due to the asymmetry of its admittance matrix. As a consequence, the methodology described in Section 3 is not valid for the integration of these devices within the DA method. However, an alternative equivalent model, which is suitable to be used with the DA method provided that slight modifications are included, is described in this section.

4.1. Pseudo pi-equivalent model

The equivalent circuit shown in Fig. 4 is still valid to represent a phase shifting transformer, provided that a is now a complex number, i.e. $a = |a|e^{j\theta}$, $|a|$ being the regulation between the primary and secondary voltage magnitudes and θ being the phase shift. The fundamental equations of such a machine can be written as

$$V_i = aV_p = a\left(\frac{B_{out}}{Y_{sc}} + V_k\right), \tag{17}$$

$$B_{out} = a^* B_{in}, \tag{18}$$

where a^* is the complex conjugate of a.

The nodal equations of a phase shifting transformer can be derived from (17) and (18) as

$$B_{in} = \frac{1}{a\,a^*} Y_{sc} V_i - \frac{1}{a^*} Y_{sc} V_k, \tag{19}$$

$$-B_{out} = -\frac{1}{a} Y_{sc} V_i + Y_{sc} V_k. \tag{20}$$

where the asymmetry of the admittance matrix becomes clear.

In order to comply with the principles of the DA method, a suitable equivalent of the phase shifting transformer should maintain the structure of (3). From (17) and (18), it can be derived that

$$V_i - V_k = \frac{a}{Y_{sc}}\left(B_{out} + \frac{a-1}{a} Y_{sc} V_k\right) = \frac{a}{Y_{sc}} B_b, \tag{21}$$

where B_b, defined as

$$B_b = B_{out} + \frac{a-1}{a} Y_{sc} V_k, \tag{22}$$

is an intermediate variable used to calculate the voltage between nodes i and k. Finally, using (17), (18) and (21), the input current to the transformer can be formulated as

$$B_{in} = e^{j2\theta}B_b + \frac{1-a}{|a|^2}Y_{sc}V_i. \quad (23)$$

The equivalent circuit shown in Fig. 6 meets the set of Eqs. (21)–(23) and constitutes the transformer phase shifting model proposed in this contribution. Though it is obviously not a pure pi-equivalent circuit, it is especially suited to be embedded in the DA power flow method, as is demonstrated in the following.

4.2. Integration of the model in the DA method

Slight modifications in the application of the DA method have to be conducted in order to integrate the pseudo pi-equivalent circuit of the phase shifting transformer into the DA power flow calculation method. The first two considerations are in fact extensions from the conclusions drawn in Section 3 for the inclusion of pi-equivalent models:

- The series impedance z_{ik} shown in Fig. 6 is used to represent the impedance between nodes i and k within the BCBV matrix.
- In the calculation of the current injection augmented vector $\boldsymbol{I}$ according to (8), $\mathbf{Y_B}$ has to include new shunt admittance terms at the sending bus, i, and receiving bus, k, according to Fig. 6.

The third consideration requires the modification of the **BIBC** matrix. As is depicted in Fig. 7(a), let i', k' and b' be the sending node, receiving node and branch index of a phase shifting transformer. In the same way, let b be the index of a branch located upstream from that transformer. According to (23) and Fig. 6, the effect of all the augmented current injections of the nodes downstream from i' on the branch current, B_b, can be evaluated as $e^{j2\theta}B_{b'}$. This fact can be easily considered by modifying the entries $BIBC_{bi}$ of the matrix. If node i is now downstream from the receiving node of branch b, the following term,

$$BIBC_{bi} = \prod_t e^{j2\theta_t} = e^{j2\sum_t \theta_t}, \quad (24)$$

applies instead of 1, with t being the different phase shifting transformers between the receiving node of branch b and node i, and θ_t being their corresponding phase angle shifts. Fig. 7 illustrates the process for the cases of one phase shifting transformer, example (a), and two series connected phase shifting transformers, example (b).

4.3. Dealing with weakly meshed grids

Additional changes, apart from those described in Section 2, must be conducted to include the proposed phase shifting transformer model in the DA method in the context of weakly meshed topologies. Those modifications can be summarized in the following aspects:

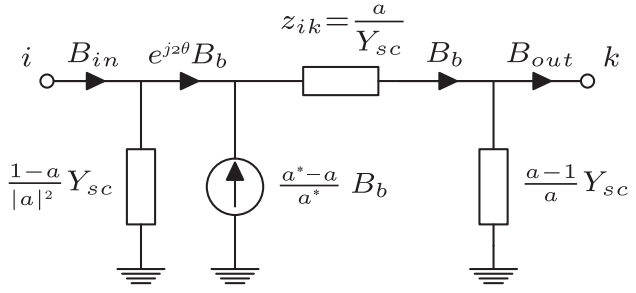

Fig. 6. Pseudo pi-equivalent model of the tap changing transformer.

- The double-sided contribution of the current of a branch used to break the network, B_c, to a branch current upstream from the first common parent node, B_b, is no longer canceled in this case, as it is shown in Fig. 8. Notice that even if B_c arises with different current references in each path, both sides can be affected by different phase angle jumps. As a consequence, a minor modification of the **BIBC** matrix is required. For those branches, b, upstream from the first common parent node, the contribution of a branch used to break the network, c, whose current branch is at position i in the augmented injection vector $[\boldsymbol{I_g B}_{\text{new}}]^T$, is evaluated by the term

$$BIBC_{bi} = \prod_{t_s} e^{j2\theta_{ts}} - \prod_{t_r} e^{j2\theta_{tr}} = e^{j2\sum_{t_s}\theta_{ts}} - e^{j2\sum_{t_r}\theta_{tr}}. \quad (25)$$

  In (25) t_s stands for the different phase shifting transformers found in the path between the receiving node of branch b and the receiving node of branch c that includes the sending node of branch c. In the same way, t_r stands for the different phase shifting transformers found in the path between the receiving node of branch b and the receiving node of branch c that does not include the sending node of branch c. Finally, θ_{ts} and θ_{tr} account for their corresponding phase angle shifts. The example shown in Fig. 8 illustrates this situation using a simple network. Notice that, in this example, one phase shifting transformer exists between node n and the receiving node k' of branch c along the path that includes the sending node of branch c. However, no phase shifting transformers exist along the alternative path connecting the same pair of nodes, which obviously leads to -1 in the second addend of (25).
- From the application of (5) and (6) to this case, it follows that

$$\begin{bmatrix}\boldsymbol{\Delta V}\\ 0\end{bmatrix}^{(n+1)} = \mathbf{BCBV}\cdot\mathbf{BIBC}\cdot\begin{bmatrix}\boldsymbol{I}\\ \boldsymbol{B}_{\text{new}}\end{bmatrix}^{(n)} = \begin{bmatrix}\boldsymbol{A} & \boldsymbol{P}\\ \boldsymbol{M} & \boldsymbol{N}\end{bmatrix}\begin{bmatrix}\boldsymbol{I}\\ \boldsymbol{B}_{\text{new}}\end{bmatrix}^{(n)}.$$

  Notice that the symmetry found in (7) does not appear in (26). In any case, the application of Kron reduction leads to

$$\boldsymbol{\Delta V}^{(n+1)} = (\boldsymbol{A} - \boldsymbol{P}\boldsymbol{N}^{-1}\boldsymbol{M})\boldsymbol{I}^{(n)}. \quad (26)$$

The iterative use of (1), (8), (26) and (4), in this order, allows the application of the DA method to weakly meshed grids including phase shifting transformers.

5. Case studies

To demonstrate the validity of the proposed methodology, three case studies are carried out in this section. In the first one, the DA method is applied to a radial network in which the phase shifts associated to the embedded power transformers are considered. In the second case study, the same radial grid is turned into a weakly meshed grid by using a phase shifting transformer. While the first two case studies take advantage of the low number of nodes of an industrial grid to give insight into the matrices building process, the third case study is used to demonstrate the good convergence characteristics of the method in a standard medium-size testbed.

5.1. Case 1: Radial network

A simplified version of the customer owned grid of a steelworks in the north of Spain, already tested in previous works [8], is considered in this case study. The grid is shown in Fig. 9 and the parameters and configuration of the embedded transformers are listed in Table 1. Table 2 shows the lengths and per km impedances

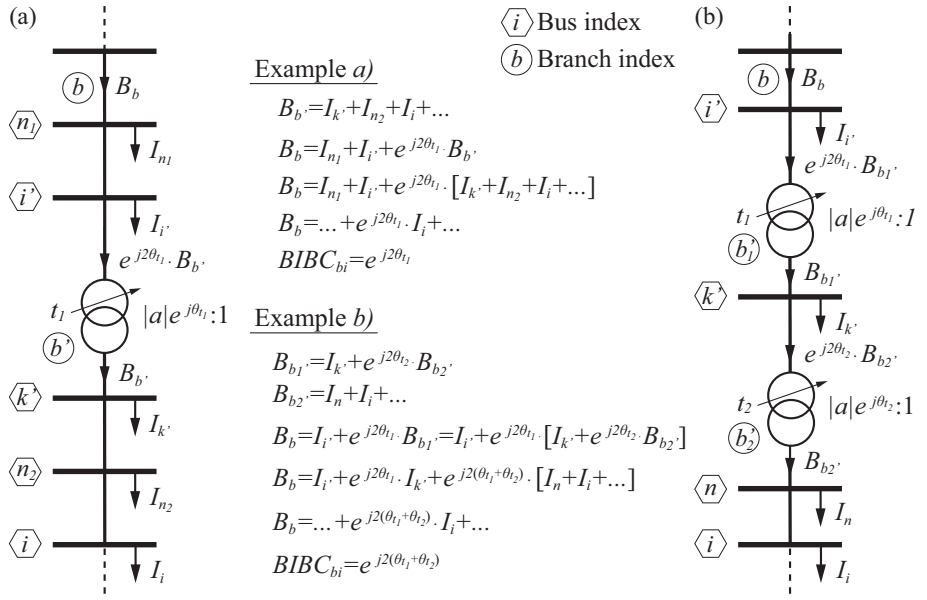

Fig. 7. Building process of the **BIBC** matrix for grids with embedded phase shifting transformers. (a) Example with one phase shifting transformer, and (b) example with two phase shifting transformers.

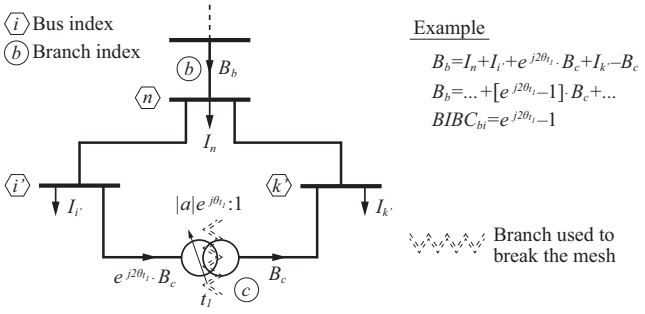

Fig. 8. Example of the building process of the **BIBC** matrix for weakly meshed grids with embedded phase-shifting transformers.

of the lines, together with the series impedances, z_{ik}, of each branch for lines and transformers, according to Figs. 2 and 6 respectively.

In [8], a proposal aimed to improve the efficiency of the grid and provide dynamic voltage support to the facility was presented. This objective is conducted through the application of a distribution FACTS usually known as Loop Power Flow Controller (LPFC). The real-time optimization of the device is based on a heuristic algorithm out of the scope of this paper. However, the proper operation of that heuristic algorithm relies upon the availability of a fast power flow algorithm, compatible with such a real-time application. Even if other algorithms were considered, the DA method shows very good performance in this environment, characterized by a small number of nodes and radial nature. The controller uses the DA power flow algorithm to analyze the effect of different power injections at the power converter terminals (i.e. the real power, P, flowing from terminal A to B in Fig. 9, and the decoupled reactive power injections at both terminals, Q_A and Q_B). The addition of these values to the rest of the power injections at buses 7 and 9 turns the power flow problem into a pure radial case, despite of the mesh created by the distribution FACTS. Table 3 shows the specific power injection values considered in this case study. Note that the negative value of the reactive power injection in bus 9 is due to the reactive power supply of the LPFC at terminal B for the current operation point. The voltage at the slack bus is taken as 1.0 pu and as the origin of phase angles.

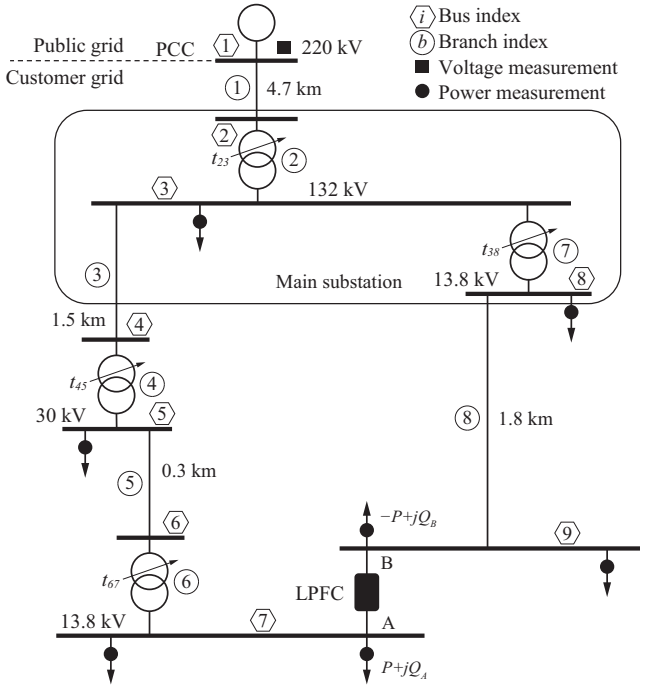

Fig. 9. Industrial installation with a distribution-FACTS-based mesh.

The use of the phase shifting model proposed in this contribution for the tapped transformers in such a radial network is not really mandatory, as it would be in Case 2. This is due to the fact that, in a radial network, the phase shift of the transformers can be initially disregarded and later taken into account on a subsequent post-processing of the results that would correct the phase angle jump in each voltage area. Nevertheless, the use of the proposed phase shifting transformer model is applied in this case study in order to avoid any post-processing of the results.

The **BIBC** and **BCBV** matrices are calculated according to the considerations disclosed in sub-Section 4.2. Their structure is shown in (27) and (28) for the sake of clarity.

$$\begin{bmatrix} 1 & e^{j2\theta_{23}} & e^{j2\theta_{23}} & e^{j2(\theta_{23}+\theta_{45})} & e^{j2(\theta_{23}+\theta_{45})} & e^{j2(\theta_{23}+\theta_{45}+\theta_{67})} & e^{j2(\theta_{23}+\theta_{38})} & e^{j2(\theta_{23}+\theta_{38})} \\ 0 & 1 & 1 & e^{j2\theta_{45}} & e^{j2\theta_{45}} & e^{j2(\theta_{45}+\theta_{67})} & e^{j2\theta_{38}} & e^{j2\theta_{38}} \\ 0 & 0 & 1 & e^{j2\theta_{45}} & e^{j2\theta_{45}} & e^{j2(\theta_{45}+\theta_{67})} & 0 & 0 \\ 0 & 0 & 0 & 1 & 1 & e^{j2\theta_{67}} & 0 & 0 \\ 0 & 0 & 0 & 0 & 1 & e^{j2\theta_{67}} & 0 & 0 \\ 0 & 0 & 0 & 0 & 0 & 1 & 0 & 0 \\ 0 & 0 & 0 & 0 & 0 & 0 & 1 & 1 \\ 0 & 0 & 0 & 0 & 0 & 0 & 0 & 1 \end{bmatrix} \quad (27)$$

$$\begin{bmatrix} z_{12} & 0 & 0 & 0 & 0 & 0 & 0 & 0 \\ z_{12} & z_{23} & 0 & 0 & 0 & 0 & 0 & 0 \\ z_{12} & z_{23} & z_{34} & 0 & 0 & 0 & 0 & 0 \\ z_{12} & z_{23} & z_{34} & z_{45} & 0 & 0 & 0 & 0 \\ z_{12} & z_{23} & z_{34} & z_{45} & z_{56} & 0 & 0 & 0 \\ z_{12} & z_{23} & z_{34} & z_{45} & z_{56} & z_{67} & 0 & 0 \\ z_{12} & z_{23} & 0 & 0 & 0 & 0 & z_{38} & 0 \\ z_{12} & z_{23} & 0 & 0 & 0 & 0 & z_{38} & z_{89} \end{bmatrix} \quad (28)$$

A flat voltage profile is considered for the initial iteration step. The set (1)–(4) is applied iteratively together with (8) to account for the augmented current injection vector, until a threshold of $1e-6$ is reached in the maximum absolute deviation of two consecutive entries in $\boldsymbol{V}$. The voltages at the different buses, as state variables of the grid, are presented in Table 4. The system has also been implemented in the PowerWorld™ Simulator software to crosscheck and demonstrate the validity of the results. Even if this tool uses a Newton-Raphson approach to solve the system, the results are identical up to the threshold level, hence their representation is avoided in this paper.

Table 1
Transformer parameters.

Transf. #	S_n [MVA]	R_{sc} [%]	X_{sc} [%]	a [pu]	θ [deg.]
t_{23}	2×270	0.90	12.90	1.0125	−30
t_{45}	3×37.5	0.90	9.00	0.9875	0
t_{67}	10	0.95	4.80	0.9250	30
t_{38}	3×50	0.92	8.50	0.9750	30

Table 2
Branch parameters.

Branch #	Length [km]	z_{line} [Ω/km]	z_{ik} [pu]
1	4.7	$0.025 + j0.240$	$2.428e-5 + j2.331e-4$
2	–	–	$1.356e-3 + j2.010e-3$
3	1.5	$0.161 + j0.151$	$1.386e-4 + j1.300e-4$
4	–	–	$7.900e-4 + j7.900e-3$
5	0.3	$0.568 + j0.133$	$1.893e-3 + j4.433e-4$
6	–	–	$-1.459e-2 + j4.285e-2$
7	–	–	$-2.245e-3 + j5.084e-3$
8	1.8	$0.161 + j0.112$	$1.522e-2 + j1.059e-2$

Table 3
Power injections.

Bus #	Real power, P_i [MW]	Reactive power, Q_i [Mvar]
2	0.0	0.0
3	84.0	26.0
4	0.0	0.0
5	34.0	12.0
6	0.0	0.0
7	4.9	12.6
8	52.0	39.0
9	2.7	−3.4

Table 4
Case 1 – Results: state variables.

Bus #	$\lvert V_i \rvert$ [pu]	θ_i [deg.]	Bus #	$\lvert V_i \rvert$ [pu]	θ_i [deg.]
2	0.9972	−0.226	6	0.9419	25.588
3	0.9579	27.278	7	0.9496	−5.097
4	0.9570	27.270	8	0.9574	−4.478
5	0.9436	25.436	9	0.9569	−4.980

5.2. Case 2: Weakly meshed grid

In this case study, the industrial network considered in the previous subsection is used to verify the correct performance of the DA method with embedded phase shifting transformers in the context of a weakly meshed grid. With this aim, a similar role as the one played by the LPFC in Case 1 is played by a tapped phase shifting transformer. This device regulates the power flow between nodes 7 and 9. The new setup is depicted in Fig. 10. The parameters and selected tap of the phase shifting transformer used to mesh the grid is shown in Tables 5 and 6 displays the series impedance, z_{79}, of the new branch according to the model shown in Fig. 6.

Only the proposal presented in this paper allows the application of the efficient DA method to this type of system. Notice that in this case a post-processing of the phase-angle jumps of the transformers is not possible, due to the coupling between both sides of the grid downstream from the first common parent node. The new branch, $c = 9$, is selected to break the mesh, though any other branch within the loop (i.e. 3 to 8) could be used with this aim. According to Section 2 and Sub-Section 4.3, once the selection is made, this branch is treated as an additional source of current injection at nodes 7 and 9. However, the use of Kron reduction allows a straightforward consideration of the mesh, i.e. no additional iterative processes are involved. For clarity purposes, the same power injections considered in Case 1 are adopted here and once again the voltage at the slack bus is taken as 1.0 pu and as the origin of phase angles.

The **BIBC** and **BCBV** matrices are calculated according to the specific considerations described in sub-Section 4.3. Their structure is shown in (29) and (30). The entries $BIBC_{19}$ and $BIBC_{29}$ account for the double contribution of B_9 to the branch currents B_1 and B_2, respectively. Notice, as an example, that for $BIBC_{19}$ the phase shifts to be considered fit $t_r = [t_{23}, t_{45}, t_{67}, t_{79}]^T$ and $t_s = [t_{23}, t_{38}]^T$. It should be highlighted that both $BIBC_{19}$ and $BIBC_{29}$ would be zero in a meshed network not including phase shifting transformers, as the contribution of both sides would be canceled upstream from the first common parent node in such a case.

$$\begin{bmatrix} 1 & e^{j2\theta_{23}} & e^{j2\theta_{23}} & e^{j2(\theta_{23}+\theta_{45})} & e^{j2(\theta_{23}+\theta_{45})} & e^{j2(\theta_{23}+\theta_{45}+\theta_{67})} & e^{j2(\theta_{23}+\theta_{38})} & e^{j2(\theta_{23}+\theta_{38})} & e^{j2(\theta_{23}+\theta_{45}+\theta_{67}+\theta_{79})} - e^{j2(\theta_{23}+\theta_{38})} \\ 0 & 1 & 1 & e^{j2\theta_{45}} & e^{j2\theta_{45}} & e^{j2(\theta_{45}+\theta_{67})} & e^{j2\theta_{38}} & e^{j2\theta_{38}} & e^{j2(\theta_{45}+\theta_{67}+\theta_{79})} - e^{j2\theta_{38}} \\ 0 & 0 & 1 & e^{j2\theta_{45}} & e^{j2\theta_{45}} & e^{j2(\theta_{45}+\theta_{67})} & 0 & 0 & e^{j2(\theta_{45}+\theta_{67}+\theta_{79})} \\ 0 & 0 & 0 & 1 & 1 & e^{j2\theta_{67}} & 0 & 0 & e^{j2(\theta_{67}+\theta_{79})} \\ 0 & 0 & 0 & 0 & 1 & e^{j2\theta_{67}} & 0 & 0 & e^{j2(\theta_{67}+\theta_{79})} \\ 0 & 0 & 0 & 0 & 0 & 1 & 0 & 0 & e^{j2\theta_{79}} \\ 0 & 0 & 0 & 0 & 0 & 0 & 1 & 1 & -1 \\ 0 & 0 & 0 & 0 & 0 & 0 & 0 & 1 & -1 \\ 0 & 0 & 0 & 0 & 0 & 0 & 0 & 0 & 1 \end{bmatrix} \quad (29)$$

$$\begin{bmatrix} z_{12} & 0 & 0 & 0 & 0 & 0 & 0 & 0 & 0 \\ z_{12} & z_{23} & 0 & 0 & 0 & 0 & 0 & 0 & 0 \\ z_{12} & z_{23} & z_{34} & 0 & 0 & 0 & 0 & 0 & 0 \\ z_{12} & z_{23} & z_{34} & z_{45} & 0 & 0 & 0 & 0 & 0 \\ z_{12} & z_{23} & z_{34} & z_{45} & z_{56} & 0 & 0 & 0 & 0 \\ z_{12} & z_{23} & z_{34} & z_{45} & z_{56} & z_{67} & 0 & 0 & 0 \\ z_{12} & z_{23} & 0 & 0 & 0 & 0 & z_{38} & 0 & 0 \\ z_{12} & z_{23} & 0 & 0 & 0 & 0 & z_{38} & z_{89} & 0 \\ 0 & 0 & z_{34} & z_{45} & z_{56} & z_{67} & -z_{38} & -z_{89} & z_{79} \end{bmatrix} \quad (30)$$

As in the previous case study, a flat voltage profile is considered for the initial iteration step. The set (1), (8), (26) and (4) is applied iteratively in this order until convergence. With this aim, a threshold of $1e-6$ in the maximum absolute deviation of two consecutive values in $\boldsymbol{V}$ is considered. The solution of the power flow problem, in the form of the bus voltages taken as state variables of the system, is presented in Table 7. The new setup was also implemented in the PowerWorld™ Simulator software package to demonstrate the validity of the results. As in the previous case study, those results are not showed here, due to a perfect match with the proposed methodology.

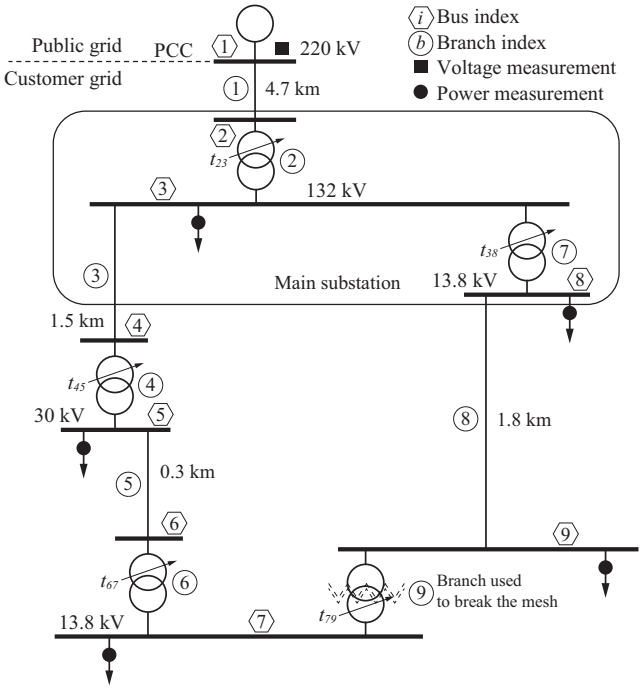

Fig. 10. Industrial installation meshed through a phase shifting transformer.

Table 5
Phase shifting transformer parameters.

Transf. #	S_n [MVA]	R_{sc} [%]	X_{sc} [%]	a [pu]	θ [deg.]
t_{79}	10	0.95	4.80	1.0000	5

Table 6
New branch parameters.

Branch #	Length [km]	z_{line} [Ω/km]	z_{ik} [pu]
9	–	–	$5.280e-3+j4.865e-2$

Table 7
Case 2 – Results: state variables.

Bus #	$\lvert V_i \rvert$ [pu]	θ_i [deg.]	Bus #	$\lvert V_i \rvert$ [pu]	θ_i [deg.]
2	0.9972	−0.223	6	0.9423	25.955
3	0.9578	27.275	7	0.9485	−2.824
4	0.9569	27.273	8	0.9574	−4.714
5	0.9428	25.766	9	0.9478	−5.775

5.3. Case 3: Standard test grid

The IEEE 33-bus test distribution system [17] is used in this case study to assess the impact of the inclusion of the proposed phase shifting transformer model on the convergence characteristics of the DA method. This standard testbed describes a radial grid with 33 buses and 5 tie lines. A modified version of this testbed is presented in this contribution in order to test the proposed model. The modified version, shown in Fig. 11, uses two of the existing tie lines to mesh the network through phase shifting transformers. With this aim, two additional buses, 34 and 35, are added to the standard system. The power injections and line parameters of the IEEE 33-bus test distribution system can be found in [17]. The parameters of the phase shifting transformers, which are the only data of the modified topology not presented in the original testbed, are shown in Table 8.

While the original version is solved using the traditional DA formulation [7], only the proposal included in this paper allows the DA method to solve the modified testbed. The results for both cases are shown in Tables 9 and 10. The validity of these results was checked by using PowerWorld™ Simulator software. System losses are reduced from 211.00 kW to 183.14 kW thanks to the control of the power flows offered by the use of phase shifting transformers. Furthermore, the minimum bus voltage in the grid increases from 0.9038 pu to 0.9203 pu, which illustrates the voltage support capability of the modified topology. A threshold of $1e-6$ in the maximum absolute deviation of two consecutive values in $\boldsymbol{V}$ was considered and, starting from a flat voltage profile,

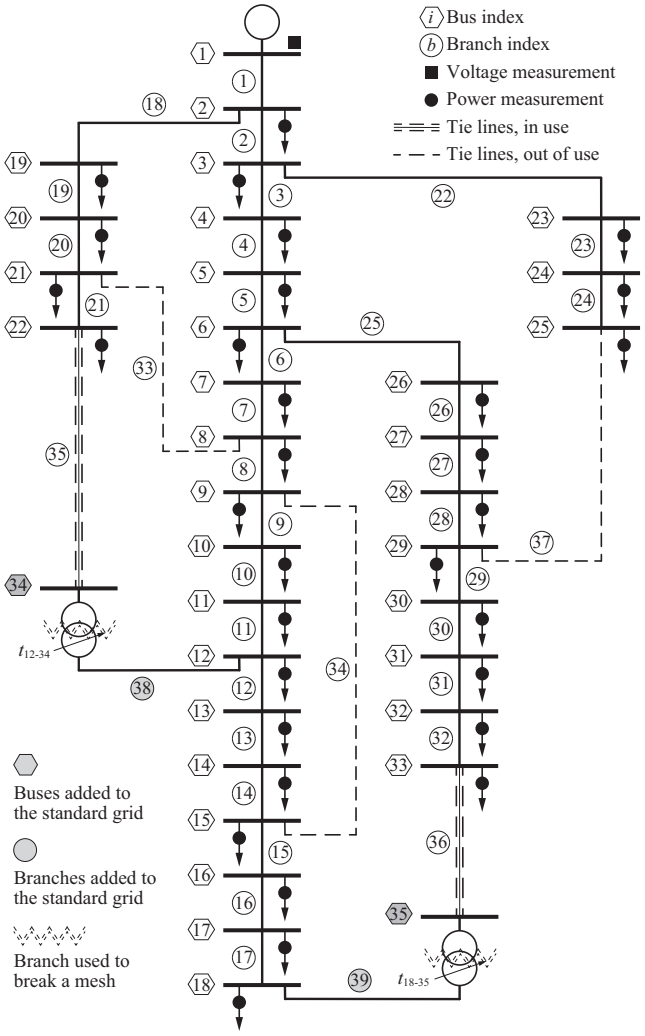

Fig. 11. Modified IEEE 33-bus test distribution system.

Table 8
Phase shifting transformer parameters.

Transf. #	S_n [kVA]	R_{sc} [%]	X_{sc} [%]	a [pu]	θ [deg.]
t_{12-34}	250	0.95	4.80	1.0000	5
t_{18-35}	400	0.95	4.80	1.0000	−3

Table 9
Case 3 – IEEE 33-bus system: state variables.

Bus #	$\lvert V_i \rvert$ [pu]	θ_i [deg.]	Bus #	$\lvert V_i \rvert$ [pu]	θ_i [deg.]
2	0.9970	0.015	19	0.9965	0.004
3	0.9829	0.097	20	0.9929	−0.063
4	0.9754	0.163	21	0.9922	−0.083
5	0.9680	0.230	22	0.9916	−0.103
6	0.9495	0.136	23	0.9793	0.066
7	0.9460	−0.096	24	0.9726	−0.023
8	0.9323	−0.249	25	0.9693	−0.067
9	0.9260	−0.324	26	0.9475	0.175
10	0.9201	−0.388	27	0.9450	0.232
11	0.9192	−0.380	28	0.9335	0.315
12	0.9177	−0.368	29	0.9253	0.393
13	0.9115	−0.462	30	0.9218	0.498
14	0.9092	−0.542	31	0.9176	0.413
15	0.9078	−0.580	32	0.9167	0.390
16	0.9064	−0.604	33	0.9164	0.383
17	0.9044	−0.683	34	–	–
18	0.9038	−0.693	35	–	–

Table 10
Case 3 – Modified IEEE 33-bus system: state variables.

Bus #	$\lvert V_i \rvert$ [pu]	θ_i [deg.]	Bus #	$\lvert V_i \rvert$ [pu]	θ_i [deg.]
2	0.9970	0.016	19	0.9959	−0.010
3	0.9845	0.116	20	0.9873	−0.204
4	0.9781	0.196	21	0.9851	−0.275
5	0.9719	0.277	22	0.9819	−0.401
6	0.9562	0.263	23	0.9809	0.085
7	0.9537	0.088	24	0.9742	−0.003
8	0.9445	−0.043	25	0.9709	−0.047
9	0.9409	−0.104	26	0.9544	0.313
10	0.9377	−0.155	27	0.9520	0.384
11	0.9372	−0.154	28	0.9412	0.545
12	0.9365	−0.154	29	0.9334	0.683
13	0.9296	−0.347	30	0.9302	0.815
14	0.9272	−0.480	31	0.9266	0.814
15	0.9255	−0.563	32	0.9258	0.821
16	0.9237	−0.637	33	0.9255	0.853
17	0.9213	−0.847	34	0.9750	−0.605
18	0.9203	−0.909	35	0.9257	0.896

Table 11
Convergence characteristics: set of 10,000 simulations.

Topology	Av. iter. #	Max. iter. #	Av. sim. time [ms]
Base case	6.0244	7	1.4019
Modified version	5.9528	7	3.5503

only 6 iterations were needed to reach convergence in both topologies. This fact proves that the excellent convergence characteristics of the DA method persist with the inclusion of the proposed phase shifting transformer model.

In order to generalize this result, a set of 10,000 cases was solved with the aim of putting additional stress on the convergence test. With this purpose, the power injections of the 33-bus testbed were randomly varied using independent normal distribution functions for each real power and reactive power. The mean of these distribution functions was set to their corresponding values in the original testbed, P_i and Q_i, and the standard deviation to 40% of these values, i.e. $N(P_i, (0.4P_i)^2)$ and $N(Q_i, (0.4Q_i)^2)$. The set was solved by applying the traditional DA formulation to the original testbed topology, and by applying the formulation proposed in this paper to the modified topology. Table 11 shows the key results of this demanding test. The average and maximum number of iterations were not increased by the use of the phase shifting transformer model even when the meshed configuration used in the modified version results in a more complex topology. In fact, the average number of iterations is slightly reduced, as the voltage support capability of the phase shifting transformers leads to solutions closer to the flat voltage profile used as an initial iteration point. The time required for these calculations was estimated by averaging the results over the full set of simulation runs, which were carried out in an Intel Core i5 - 2467M - CPU 1.60 GHz. This time increases from 1.4 ms to 3.6 ms, which is due to the higher number of buses used in the modified topology, 35 vs. 33, and particularly, to the additional matrix manipulations involved in the treatment of meshed grids, according to Subsection 4.3. This test clearly demonstrates that the convergence characteristics of the DA method are not negatively affected by the inclusion of the phase shifting model proposed in this contribution.

6. Concluding remarks

This paper proposes an extension of the well-known DA power flow method applied to balanced networks in order to allow its use

with common grid components not previously considered in the existing formulation. The inclusion of pi-equivalent line models and transformer tap changers is quite straightforward, and only a formal formulation of the considerations needed to use these components is stated in this work. However, the inclusion of phase shifting transformer models in the DA method is far from obvious, due to the inherent asymmetry of their admittance matrix. Only a custom model of these devices can allow the application of the DA method in weakly meshed networks, where the phase angle of transformers cannot be corrected by post-processing. Thus, this proposal introduces a new phase shifting transformer model, together with a set of slight modifications to be included in the standard DA power flow formulation. Two case studies in the context of the application of fast power flow algorithms to industrial networks are presented. Those cases allow to demonstrate the validity of the proposal both with radial and weakly-meshed topologies. A third case study is carried out in a medium-size test system in order to prove that the excellent convergence characteristics of the DA method are not deteriorated by the inclusion of the new phase shifting transformer model. In each case, the results are compared with those obtained from a popular software package that uses a different approach, leading to a perfect match.

Acknowledgment

This work was supported by the Spanish Ministry of Economy and Competitiveness through the National Plan for Scientific and Technical Research and Innovation under grant ENE2014-52272-R.

References

[1] Gómez-Expósito A, Conejo AJ, Cañizares C. Electric energy systems: analysis and operation. 1st ed. Boca Raton, FL: CRC Press LLC; 2009.
[2] Martinez JA, Mahseredjian J. Load flow calculations in distribution systems with distributed resources: a review. In: 2011 IEEE power and energy society general meeting. p. 1–8. http://dx.doi.org/10.1109/PES.2011.6039172.
[3] Das D, Kothari DP, Kalam A. Simple and efficient method for load flow solution of radial distribution networks. Int J Electr Power Energy Syst 1995;17(5):335–46. http://dx.doi.org/10.1016/0142-0615(95)00050-0.
[4] Chen TH, Chen MS, Hwang KJ, Kotas P, Chebli EA. Distribution system power flow analysis-a rigid approach. IEEE Trans Power Deliv 1991;6(3):1146–52. http://dx.doi.org/10.1109/61.85860.
[5] Shirmohammadi D, Hong HW, Semlyen A, Luo GX. A compensation-based power flow method for weakly meshed distribution and transmission networks. IEEE Trans Power Syst 1988;3(2):753–62. http://dx.doi.org/10.1109/59.192932.
[6] Kersting WH. Distribution system modeling and analysis. 1st ed. Boca Raton, FL: CRC Press LLC; 2002.
[7] Teng J-H. A direct approach for distribution system load flow solutions. IEEE Trans Power Deliv 2003;18(3):882–7. http://dx.doi.org/10.1109/TPWRD.2003.813818.
[8] Cano JM, Norniella JG, Rojas CH, Orcajo GA, Jatskevich J. Application of loop power flow controllers for power demand optimization at industrial customer sites. In: 2015 IEEE power energy society general meeting. p. 1–5. http://dx.doi.org/10.1109/PESGM.2015.7285766.
[9] Bandler J, El-Kady M, Grewal H. An application of complex branch modeling to nonreciprocal power transmission elements. IEEE Trans Circ Syst 1985;32(12):1292–5. http://dx.doi.org/10.1109/TCS.1985.1085671.
[10] Jimenez JC, Nwankpa CO. Circuit model of a phase-shifting transformer for analog power flow emulation. In: 2011 IEEE international symposium of circuits and systems (ISCAS). p. 1864–7. http://dx.doi.org/10.1109/ISCAS.2011.5937950.
[11] Youssef RD. Phase-shifting transformers in load flow and short-circuit analysis: modelling and control. IEE Proc C – Gener Transm Distrib 1993;140(4):331–6. http://dx.doi.org/10.1049/ip-c.1993.0049.
[12] Acha E, Ambriz-Perez H, Fuerte-Esquivel CR. Advanced transformer control modeling in an optimal power flow using Newton's method. IEEE Trans Power Syst 2000;15(1):290–8. http://dx.doi.org/10.1109/59.852135.
[13] Nabavi Niaki SA. A novel steady-state model and principles of operation of phase-shifting transformer comparable with FACTS new devices. Proceedings of international conference on power system technology, vol. 3. p. 1450–7. http://dx.doi.org/10.1109/ICPST.2002.1067770.
[14] Tziouvaras DA, Jimenez R. 138 kV phase shifting transformer protection: EMTP modeling and model power system testing. 2004 Eighth IEE international conference on developments in power system protection, vol. 1. p. 343–7. http://dx.doi.org/10.1049/cp:20040133.
[15] Okon T, Wilkosz K. Phase shifter models for steady state analysis. In: 2016 17th International scientific conference on electric power engineering (EPE). p. 1–6. http://dx.doi.org/10.1109/EPE.2016.7521831.
[16] Barboza LV, Zürn HH, Salgado R. Load tap change transformers: a modeling reminder. IEEE Power Eng Rev 2001;21(2):51–2. http://dx.doi.org/10.1109/MPER.2001.4311274.
[17] Baran ME, Wu FF. Network reconfiguration in distribution systems for loss reduction and load balancing. IEEE Trans Power Deliv 1989;4(2):1401–7. http://dx.doi.org/10.1109/61.25627.